Photophosphorylation generates ATP committed by evolution to a central role in energy transduction to operate open systems

Dr. Alfred Bennun
Full Professor Emeritus of Biochemistry
Rutgers University

Abstract

Pioneering research in the structure and function of enzyme membrane systems, which are coupled to energy sources, could bypass the microscopic reversibility principle, and allow the emergence-development of a mechanism for vectorial kinetics. The research on the mechanism of coupled systems involved the isolation and reconstitution of the purified CF_1-ATPase with the residual membrane. Photophosphorylation involves coupling with photosystem I and II, which by uncoupling show a light-dependent and light-triggered ATPases. The isolated and then purified enzyme was also investigated as a dark functional enzyme by activation through to trypsin or heat treatment. In addition, were investigated the requirements of model mechanism, which requires microscopic physics or/and quantum mechanics level to demonstrate an energy transduction participation. This approach involved the links to the excitation states and mechanisms of photosystem I and II discovered by many other investigators. The interpretation of models using the mechanism of H-bond breakdown in the configuring of the mass-action potential by the high molarity of the water cluster allowed a far away displacement of equilibrium to the parameter ensuring irreversibility of the system. H-bond lacking molecules of water were proposed to act as dissipative carriers of entropy. Homeostatic temperature mechanisms were developing for brains. Independently of different proposals it is emphasized that fit requirements to operate life as an open system. The proposal to implicate in an overall general role of the state transition of water rather than described specifically every reaction lead to evaluate the dissipative potential of water cluster $(H_2O)n$ to interact with the hydrophilic vs hydrophobic asymmetries, which restrict randomness of in the singleness of kinetic sense. Thus, interpret its action as if it constitutes a single peak, consolidating its operative role as is activation energy (Ea). The hydration shells could in sequence act as a diffuse enhancer of specific contribution to obtain Ea of the totality of the system even as an input into several peaks that sequentially activate transition states. Hence, changes in dipole state, sliding, pKa, n-H-bonds, etc., could become concatenated for vectoriality. $(H_2O)n$ by the loss of H-bonds coupled with the hydration turnover of proteins and ions to result in incomplete water cluster $(H_2O)n^*$, with a lower-n. $(H_2O)n^*$ became a carrier of heat/entropy. The beta-scintillator batteries using Sr-89 and Sr-90 allow night agriculture and contribute to the Mars colonization projects.

Introduction

A link between microscopic and macroscopic physics may be rebelled by cosmology. The usual prevalent approach fixes the Planck units as a delimiting. The inflation role for uniform development of the cosmos could be described through the entanglement of bosons with the property to occupy the same quantum state. The latter prevents random dominance (chaos).

Life defines the temperature and pressure parameters to configure a thermodynamic, correlating structure and function for self-integration into evolution, which seeks Darwinian adaptive differentiation.

If projected into cosmology, vectorial kinetics could be the result of self-organizing principles or causality interconnection for a development chronology. Self-regulation could modify the dynamics of events, resulting in coupling of forces.

The relativistic velocities the particles acquire impulse, which in order to decrease the lineal tendency of mass increase acquire angular momentum curving trajectory. Therefore favors the concept of the dynamics of vectorial kinetics.

Thus, results in an event which provides feedback, modulating changes into a self-contained universe. Thus, causality integrates both action and reaction similarly to a biological feedback that contains information about the state of the system.

The expansion involves structure and function mechanism like a restriction of entropy within a self-contained universe. Hence, thermodynamics of transition states could function as a bottleneck to excitation states because of the fragility of an organic system, a manifestation of structure and function of thermodynamics solutions.

Life had to develop a system that captures the energy of the sun at normalized temperature rather than depending on the effect of the sun's energy to vaporize water. Accordingly, the acquired function of photosynthesis depend of decomposition of water into oxygen released to air and releasing flux of electron into electron carriers, involved in reducing by H transfer oxaloacetate, which allows the formed malate to contribute to the capture of CO_2, which is fed into the Calvin-Benson cycle.

Blue light energy is sufficient for an electron to obtain the excited singlet state, but this one decays rapidly, by loss of some energy, to form a longer-lived, first excited state. The energy of the red photon (680nm=1.82eV) activates the Photosystem II (PSII).

The green light photons are not absorbed, but are reflected, because they could not take a valence electron to an excited state.

Chlorophyll absorbs red light for an electron to occupy the first lowest and unoccupied molecular orbital of the next second lowest. Thus, the absorbed red light corresponds to the transition up to the first excited singlet state.

Most chlorophyll are bound to antenna or reaction center proteins where they play light-collecting roles, rapidly passing its excitation to one of the adjacent chlorophylls and interacts with a large number of chlorophylls during the fluorescence lifetime of about 5 nanoseconds [1].

Penrose and Hameroff [2] (they dubbed Orch-OR: orchestrated objective reduction) have argued that consciousness is the result of quantum effects in microtubules [3] [4]. Max Tegmark [5] calculated that the time scale of neuron firing and excitations in microtubules is slower than decoherence time by a factor of at least 10^{10} to allow free will implementation by 10^{11} neurons in the bases of very large presence of microtubules. Biologically, free will (*software*) is 40% indirectly resulting from the neuronal DNA (*hardware*) programmed behavior. It has been proposed that the result from infants manifest a functional amygdala and hippocampus when they still have an under-developed frontal brain. Emotional learning allows us to bypass genetic restrictions to obtain a self-cognitive level, which links to family and society experience at the unconscious level [6].

In molecular terms the microtubules space polarity allows the spins associated to maintain a dimer state. The dissociation mechanism in the brain became manifest when arriving at the oral cavity and exhaled as vapor. At homeostatic temperature dimers lacking H-bond could still be attracted by the polarity of isomers in resonance states, which allows trap entropy.

The light reactions occur in the chloroplast thylakoid membrane and involve the splitting of water into oxygen, protons and electrons. The protons and electrons are then transferred through the thylakoid membrane to create the energy storage molecules adenosine triphosphate (ATP) and nicotinomide–adenine dinucleotide phosphate (NADPH). The ATP and NADPH are then utilized by the enzymes of the Calvin–Benson cycle (the dark reactions), which convert CO_2 into carbohydrate in the chloroplast stroma [7].

Malate generated in the chloroplasts is oxidized and decarboxylated (loses CO_2) by malic enzymes. This yields high concentrations of carbon dioxide, which is fed into the Calvin-Benson cycle of the bundle sheath cells, and pyruvate, a three-carbon acid that is translocated back to the mesophyll cells.

Results

Chlorophyll fluorescence is light re-emitted by chlorophyll molecules during return from excited to non-excited states. Excited chlorophyll dissipates the absorbed light energy by driving photosynthesis (photochemical energy conversion), as heat in non-photochemical quenching or by emission as fluorescence radiation [8].

This occurs when electron acceptors downstream of PSII have not yet passed their electrons to a subsequent electron carrier, so are unable to accept another electron.

The excitation arrives at specific chlorophyll at the reaction center, its excitation energy the electron, denominated as the primary electron donor, involved in the first charge separation.

The excitation state leads to form a pair of oppositely charged radicals and the rapid electron

transfer, out from the highly reducing anion radical into the highly oxidizing cation radical.

The radiationless transitions include quantum tunneling for ultra-fast charge separation with decreasing temperature, with harmonics of vibrational relaxation occurring rapidly relative to electron transfer as its energy $E = h.\omega$.

The excited state of P [9] [10] [11] [12] may represent collective nuclear motions of the pigments and their surroundings, by a pump-probe operated in femtoseconds (fs: 10^{-15} s).

Rhodobactersphaeroides R-26 excitation of the accessory BChl (populating the excited state, B*) provides a detailed answer for the mechanism of energy transfer within the bacterial reaction center. The process proceeds via a two-step mechanism, flowing sequentially from B* to Py+ to Py- with time constants of 120 and 65 fs, respectively. Under broad-band excitation it was possible to create electronic coherence between the two exciton states $(P^*)_+$ and (P^*) [13]. The coherent motion of the exciton wave packet resulted in oscillations of the anisotropy with a frequency of 593 cm^{-1} (which is close to the exciton splitting) and damping constant of 35 fs.

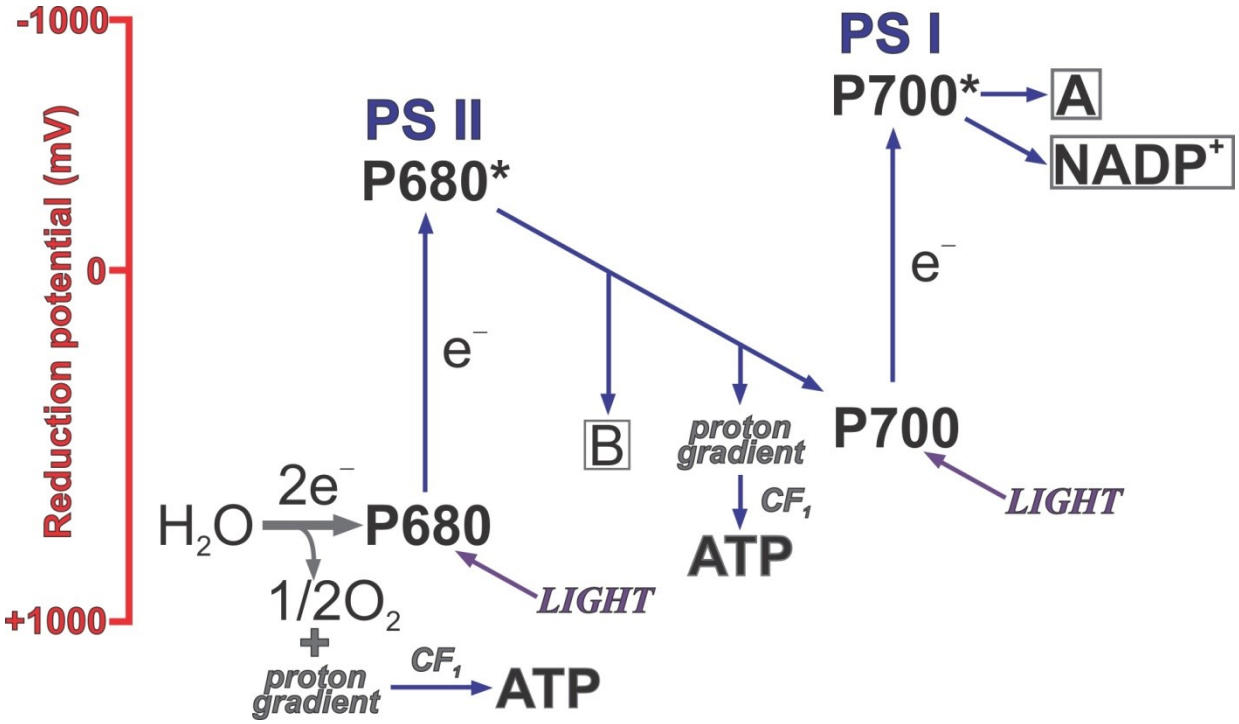

Figure 1: scheme for charge separation in photosynthetic reaction centers. *A symmetry axis runs through the centrally leaded "special pair" of BChl molecules and the pigments are organized in two branches: A and B. This occurs only along the A branch.*

Light harvesting [14] was demonstrated under light saturation involving hundreds of chlorophylls to reduce one molecule of CO_2.

Photosystem I typically work in series with Photosystem II, which have their own distinct reaction centers, named $P700^+$ and $P680^+$, respectively. These centers are named after the wavelength (in nanometers) of their red-peak absorption maximum.

Thus, the $P700^+$ of Photosystem I is usually reduced as it accepts the electron, via many intermediates in the thylakoid membrane, by electrons coming, ultimately, from Photosystem II. Electron transfer reactions in the thylakoid membranes are complex, however, and the source of electrons used to reduce $P700^+$ can vary.

Reaction center chlorophyll–protein complexes are capable of directly absorbing light and performing charge separation events without the assistance of other chlorophyll pigments, to increase the probability other chlorophylls, called accessory pigments, in the photosystem and antenna pigment proteins absorb and funnel light energy to the reaction center.

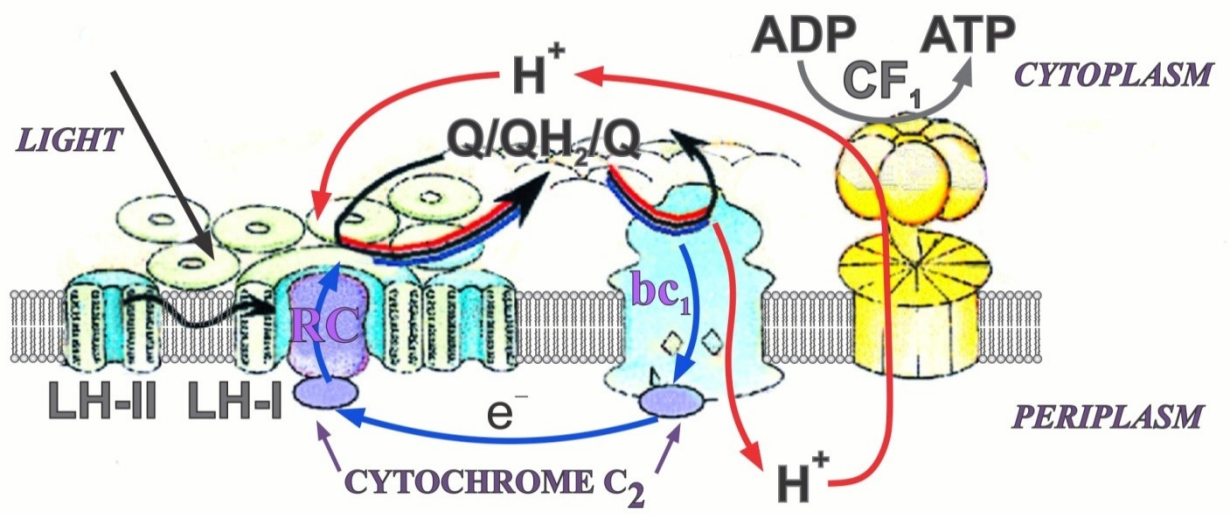

Figure 2: *A few chlorophylls constitute the primary photosynthetic reaction center (RC). Most chlorophyll serves as light-harvesting antennae by capturing the sunlight and funneling electronic excitation toward the RC. An ensemble of an RC with associated light-harvesting system constitutes the photosynthetic unit (PSU) up to 250 chlorophylls.*

A light harvesting antenna within several 10^{-12}s , without including intermediate states could be calculated:

$$CO_2 + 2H_2{}^{18}O \overset{light}{\Longrightarrow} (CH_2O) + {}^{18}O_2({}^{18}O = {}^{18}O)$$

The generated oxygens are only from water.

Fraunhofer single slit diffraction shows that the diffracted light manifests the presence of an angular momentum, allowing the light to converge into the space-time.

The expression $\Delta t = \frac{d}{c}\sin\theta$ corresponds to $\frac{d}{c}$ in where "d" it is understood to represent: λ, the light wavelength since at shorter wavelength the higher energy. By narrowing the slit, the blue light responds in a photon train emerging with a dispersion angle those results in a wider band [15].

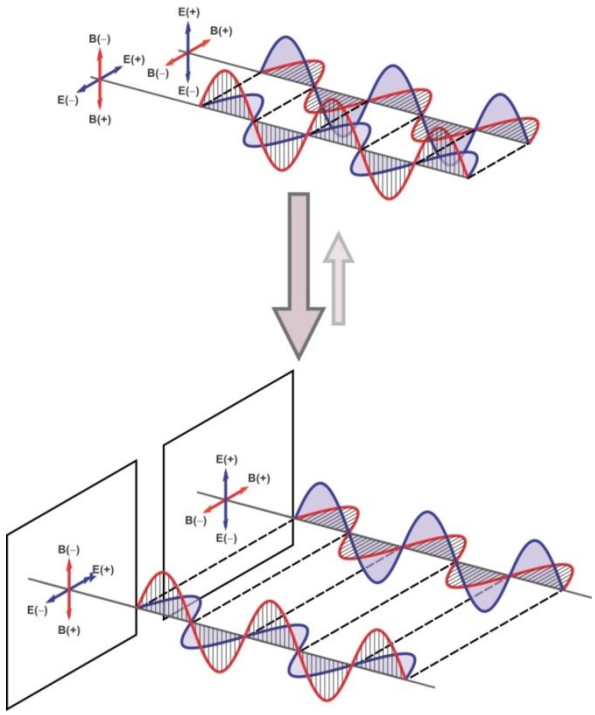

Figure 3: Quantum entanglement and photon coherence. *A pair of entangled photons integrates the fields [16], maximizing the energy density, with a minimum total angular momentum, operating as a resonance box. Decoherence implies the release of entropy.*

The orthogonal condition of the entangled photon fields [17] [18] allows an internal resonance between spins is unstable and hides a tendency for decoherence [19], and manifests a joint moment in a very small space: 10^{-9}cm. The uncertainty assay for two coherent photons results in a structure with resonance manifesting itself as a fluctuating relationship between electric vs. magnetic fields.

Quantum entanglement allows Planck bosons [20] to emerge with the same quantum state, giving homogeneity and synchronization throughout the stages of force separation. The dissipative evolution of bosons manifests cause and effect properties operating as a space-time continuum. In which, the energy decreases in frequency in a coherent state that gives homogeneity and at a low entropy rate. The system is not chaotic but self-regulating. Thus, the entropy rate ΔS [21] per time rate Δt, that is, $\frac{\Delta S}{\Delta t}$ for a self-regulating universe, it maintains a much slower rate than for a universe with many degrees of freedom [22] [23] [24].

The "two-photon" nature of the parametric down-conversion is due to the entanglement of the two photons. Two-photon coherence and two-photon entanglement are interrelated concepts. Two-photon entanglement in a given degree of freedom implies two-photon coherence in the corresponding domain. Two-photon interference experiments allow two-photon entanglement [25] [26] [27].

Werner Heisenberg's uncertainty principle [28] states that it is not possible to know position and moment with precision simultaneously: $\Delta x\, \Delta p > \frac{\hbar}{2}$ and neither can energy and time: $\Delta E\, \Delta t > \frac{\hbar}{2}$. This principle can be applied to interference and quantum entanglement.

For two entangled photons: $\Delta(2E)\, \frac{\Delta t}{2} > \frac{\hbar}{2}$, the Δt (uncertainty time) would decrease, which implies that for high frequency photons, Δt would be smaller and the location would decrease according to the expression: $\frac{\Delta x}{2}\ \Delta(2p) > \frac{\hbar}{2}$.

In quantum entanglement each photon is close enough to apply the uncertainty principle as a whole [29] [30]. This contraction of space-time imposes that the electric fields are arranged orthogonally, with the lower configuration of the energy and an increase in the density and mutually add their energetic fluidity. Thermodynamically the entangled system is subject to statistical parameters that force it to be decoherent by the flow from a higher to a lower density.

The relationship between moment (p) and total angular momentum (L) [31] [32] allows an alternative expression. Thus, $\Delta p = \frac{\Delta L}{r}$ and $\Delta x = \Delta\phi\, r$, where ϕ is the angle in radians and x is a measure of the curvature or circumference of a circle, and therefore, $\Delta L\, \Delta\phi \geq \frac{h}{4\pi}$. The latter shows the uncertainty between angular momentum (L) vs angular position (ϕ).

The total angular momentum of the system of two entangled photons would be composed mainly by the sum of their spins $L = s_1 + s_2 = 2s$. Therefore $\Delta(s_1 + s_2)\, \Delta\phi \geq \frac{h}{4\pi} \Rightarrow \Delta(2s_1)\frac{\Delta\phi}{2} \geq \frac{h}{4\pi}$. On the other hand, in a coherent photon system $\Delta(s_1)\, \Delta\phi \geq \frac{h}{4\pi}$. This allows us to conclude that $\Delta x = \frac{\Delta\phi}{2}\, r$, and therefore explains the space-time contraction of entangled photons [33].

The value of the total angular momentum of the system of two entangled photons would be less than that of a coherent photon. Therefore, due to the uncertainty principle, the dimension of the entanglement is less than the coherence.

In the interference of two photons, the superposition allows locating the position, but due to the uncertainty principle, the moment of the system cannot be known. This may have implications for the quantum entanglement of two photons. The state of the entangled pair is precisely known but the individual quantum state of each one cannot be known simultaneously. Therefore, it produces a zone of probability and superposition for the electric field to operate, which gives it a dynamic or plasticity of energetic configuration.

In the electromagnetic wave, the coherence time (τ: tau) is the time it takes to be considered coherent [34] [35], which means that its phase (T period) is predictable. Is calculated by dividing the

coherence length (is the propagation distance over which a coherent wave maintains a specified degree of coherence.) by the phase velocity of light (is the rate at which the wave propagates in some medium), approach: $\tau = \frac{1}{\Delta\nu} \approx \frac{\lambda^2}{c\Delta\lambda}$.

Where λ is the central wavelength of the source, $\Delta\lambda$ is the spectral width of the source in frequency units: $\Delta\nu$.

A single mode fiber laser has a linewidth of a few kHz, corresponding to a coherence time of a few hundred microseconds. Hydrogen masers have a linewidth around 1 Hz, corresponding to a coherence time of one second. Their coherence length corresponds to the distance from the Earth to the Moon.

For long distance transmission, the coherence time can be reduced by scattering, spreading and diffraction.

Temporal coherence is the measure of the average correlation between the value of a wave and its delay by τ, between two instants, and shows how monochromatic a source is. Thus, it characterizes how well a wave can interfere with itself at a different time.

The coherence length (L_c) is defined as the distance the wave travels in time (τ_c). At a delay of $\tau = 0$ the degree of coherence is perfect, whereas it drops significantly as the delay phases: $\tau = \tau_c$.

Photosystem II

In densely packed structures the excited states of the pigments emissions are coupled via dipole-dipole interactions.

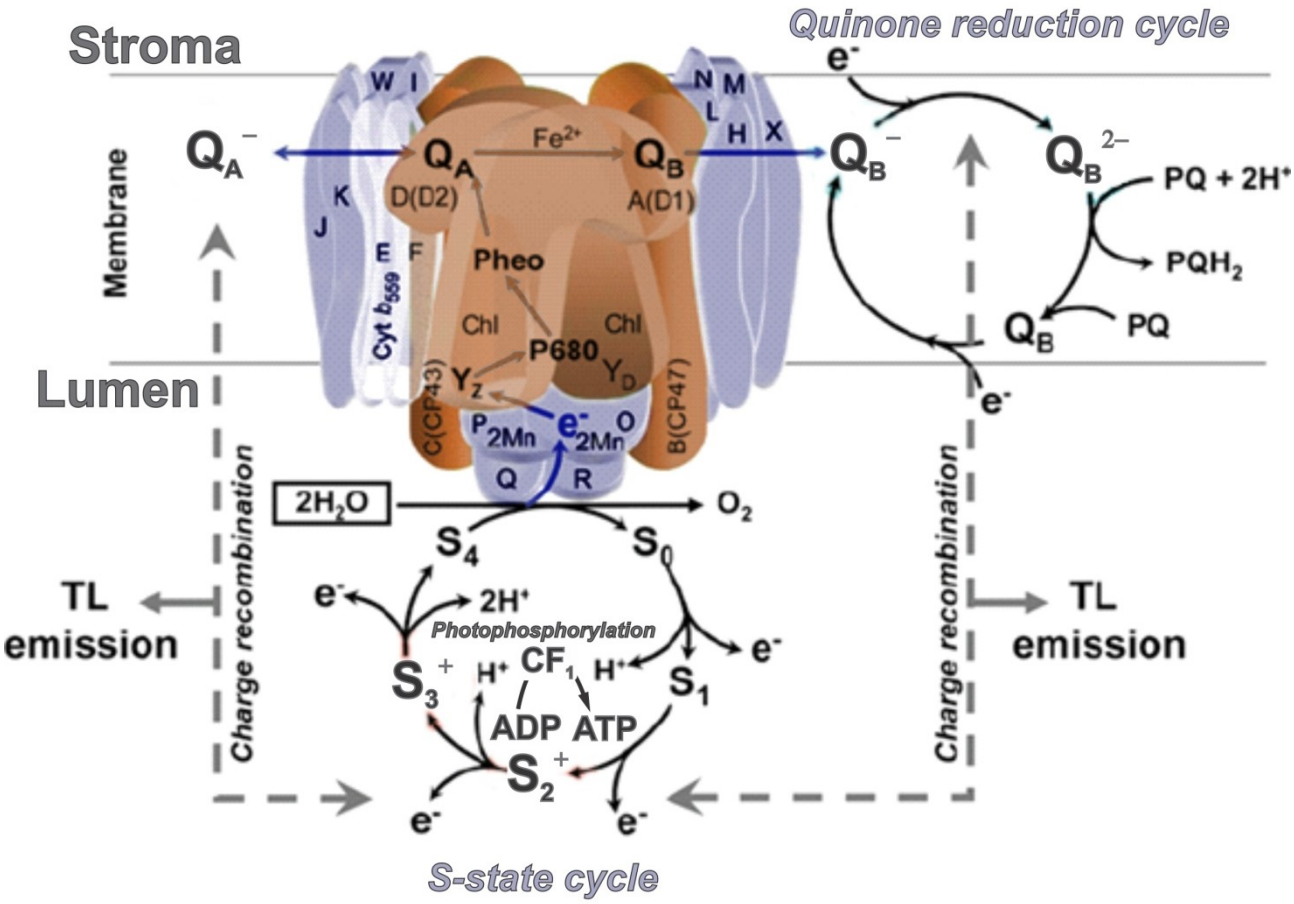

Figure 4: Polypeptide composition for electron transport carriers and light-driven photosynthetic electron transport reactions. *From Mn to the secondary quinone electron acceptor (Q) in PS B II resulting in water oxidation by the Mn cluster at the donor side of PS II.* [36]

The strength of this coupling is one of the major factors that determine how fast the excitation moves through the assembly of coupled pigments. If the dipole-dipole coupling is very weak, say much weaker than the coupling of the excited state to its environment (electron-phonon coupling).

A flux of electrons constitutes a non-polarized current, traversing a dipole oriented structure becomes polarized traveling to the structure maintaining alignment and conferring angular momentum.

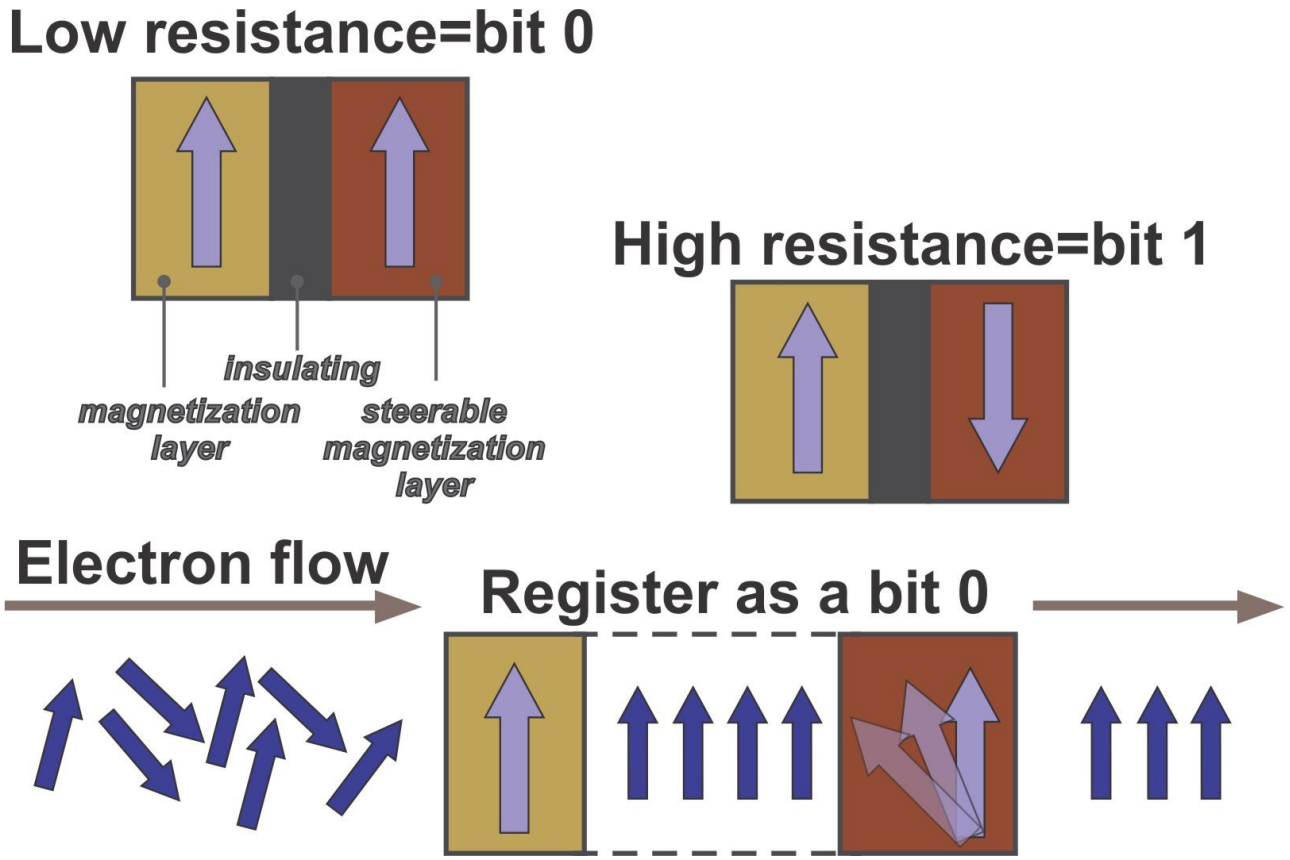

Figure 5: Polarization fields aligning spins of the electron flow. *Magnetic resistance on tunneling, an electric current flows easily, through the two magnetic configurations that lead to spins with the same sense and showing resistance when opposite spins senses result from differently oriented magnets.*

The electrogenic membrane potentials manifest selective effect on spins and decrease noise interferences. In chloroplast but more prominently clarifies signals transmission by ionic potentials fluctuation, allowing greater efficiency to neuronal circuits [37] [38].

Quantum coherence and photosynthetic light harvesting

Dipolar couplings between localized excited states not only delocalize the excited state, also 'coherences' are generated, meaning that products such as $c_i c_j^*$ have a value that may give rise to oscillatory dynamics, according to the initial excitation conditions. The adjusting stages manifest .

coherences. The excitation localization allows oscillations between pigment domains of about 60fs.

In an experiment at cryogenic temperatures [39] long-lived energy coherences up to 500 fs has been detected and were observed to occur among the exciton states of the FMO complex.

In light-harvesting complexes of cryptophytes long-lived coherences in such a noisy environment could be observed at room temperature, suggesting a role of the structure and function of the protein allowing these coherences. Specific domains may relate to hydrophilic vs hydrophobic configuration for the excitation energy transport process and capture in the reaction center.

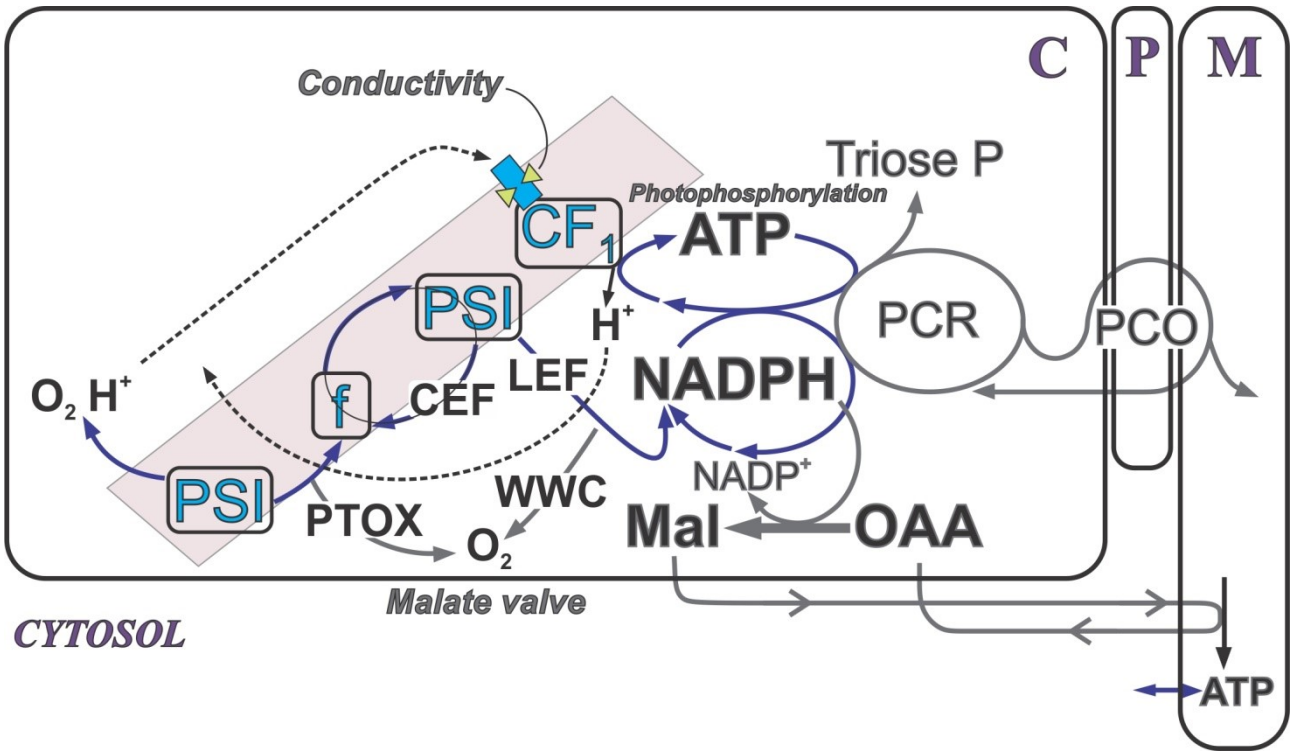

***Figure 6: The coupling between light capture, electron flow, and photophosphorylation**, which produce NADPH and ATP with their consumption by CO_2 assimilation (photosynthetic carbon reduction [PCR]) and photorespiration (photosynthetic carbon oxidation [PCO]) in a cell.*

The photosynthetic electron transport chain is represented in a thylakoid membrane, with electron flow from water through PSII, the cytochrome b/f complex (f), and PSI to NADPH, and proton flow into the lumen and out through the ATPase (CF1) to generate ATP [40].

The path for electron flow relates structure and function. Electrons can leave from PQH 2 via the plastoquinol oxidase (PTOX), which oxidizes plastoquinol and reduces oxygen to water. Some electrons can be exported from the chloroplast via the oxaloacetate (OAA) input in malate (Mal) and the dehydrogenation generating a NADPH cycle releasing $NADP^+$. The mitochondrial function to relate aerobic respiration and acetate input into the Krebs cycle were separately studied [41] [42] [43] [44].

The photons delivered to PSII reflect the relative amounts of chlorophyll associated with the two photosystems. State transitions can dissociate chlorophyll protein complexes from PSII, which may contribute to PSI, thereby enabling greater cyclic electron flow. The conductivity of the ATPase can be varied to alter the luminal pH relative to the rate of ATP synthesis, thus providing feedback via the qE quenching mechanism [45], which is activated by low pH in the lumen, reduces the effective efficiency of the antenna.

The chloroplast coupling factor 1 (CF1)

When attached to the membrane the chloroplast coupling factor (CF_1) seems to undergo a high-energy-induced conformational change to operate photophosphorylation, without any detectable reversibility.

The chloroplast's studies showing the vector of kinetic for $CF`_1$ coupling as ATP synthase, but not showing any reversibility for photophosphorylation because only from uncoupling effect could be demonstrated the ATPase functions.

Thus, under coupling conditions CF_1 in the intact chloroplast was in apparent contradiction with the principle of microscopic reversibility. The impossibility to differentiate between hot- and cold-molecules allowed a humorous description by Maxwell that the operators of a single door, capable of doing so, should be called demons.

Figuratively, the principle describes that a single microscopic door allows transit in both senses, allowing only a closed thermodynamic system, which only allows changes by mass-action equilibrium. However, an irreversible open system does have vectorial kinetics as long as enthalpy input is continuous as light trapping by the

chloroplast and entropy generated is continuously dissipated.

By bypassing the microscopic reversibility principle, illustrated as a single door, vectorial kinetics was demonstrated as possible by the assumption that it has to be two or more enzymatic coupled states (equivalent to an excess of two doors), which could allow these protein stages to operate vectorial kinetics.

Hence, alone or associated a search for a mechanism able to operate [46] like two or more interlock transition state lead to hypothesis of conformational changes described are operating when one domain is hydrophilic and the other turns to become hydrophobic, generalized like two inversely linked doors, *mutually exclusive*, one to be open when the other is closed.

Vectorial kinetics is conferred by proline-dependent polypeptide folding dynamics. The H-bonds could be regarded as doors, when open attracts water clusters to the segment containing negative R groups capable of coordinating Mg^{2+} (first door).

This hydrophilic configuration has to be mutually exclusive by H-bonds breakdown (a second door) to reconfigure a hydrophobic structure of positive R groups to attract negatively charged molecules like ADP^{3-} and inorganic phosphate to result in the endergonic product: ATP^{4-}. Hence, could not be liberated from a hydrophobic closing environment, which allows water cluster to function by H-bond breakdown of intermediate conformational changes, for vectorial decrease in the energy input from other sources.

The hydrophilic action of the very larger mass action of water clusters pulls the reaction far away from any tendency to equilibrium, and therefore, the steps tend to operate as irreversible kinetic, and the thermodynamics of photosynthesis will operate as an open system. Turnover requires the mass-action of a water cluster for additional H-bond breakdown, reconfiguring an obligatory Mg^{2+} site in CF_1 characterizing the hydrophilic state.

These are transitions thermodynamically coupled between an exergonic reaction couples to drive the endergonic, sliding event by the H-bonds breaking of the binding folding and them re-folding allow a dissipative heat release (entropy).

The directionality would be given by mutual exclusion and this complementarity would be the conformational change of the protein, dependent on a breakdown of a small ratio of H-bonds of the total potential of the water cluster [47] [48] [49]. A subsequent event depends on the exergonic uphill event of H-bond breakdown to recreate the hydrophilic domain (3th door). However, this step has the large contribution to the enthalpy of the system by a natural coupling to the high H-bond mass action of water clusters at molar level. The system operates with the remaining H-bonds within the water cluster. This is rather not detectable since at the test tube reactants and products are at μmolar level. However, the water cluster involves the solvation energy of encompassing saturation surroundings [50] [51] [52] [53].

Experimentally the solvation tendency was measured on the activity shown by the heat activated-ATPase, determined from its maximal value assayed as basal with glycerol addition at 0% only in the presence of water clusters. The curve obtained by decreasing enzyme activity to zero is reached by adding glycerol to reach 8% concentration into the mixture [54] [55] [56] [57].

Additionally, under uncoupling conditions with cysteine-HCl in the reaction mixture it was possible to recognize a light-triggered ATPase. The earliest change of this kind described light-induced change, which permits sulfhydryl reagents to interact with the coupling factor and render it reversible and active a latent ATPase and ATP-Pi exchange reactions and markedly changes its affinity for GTP.

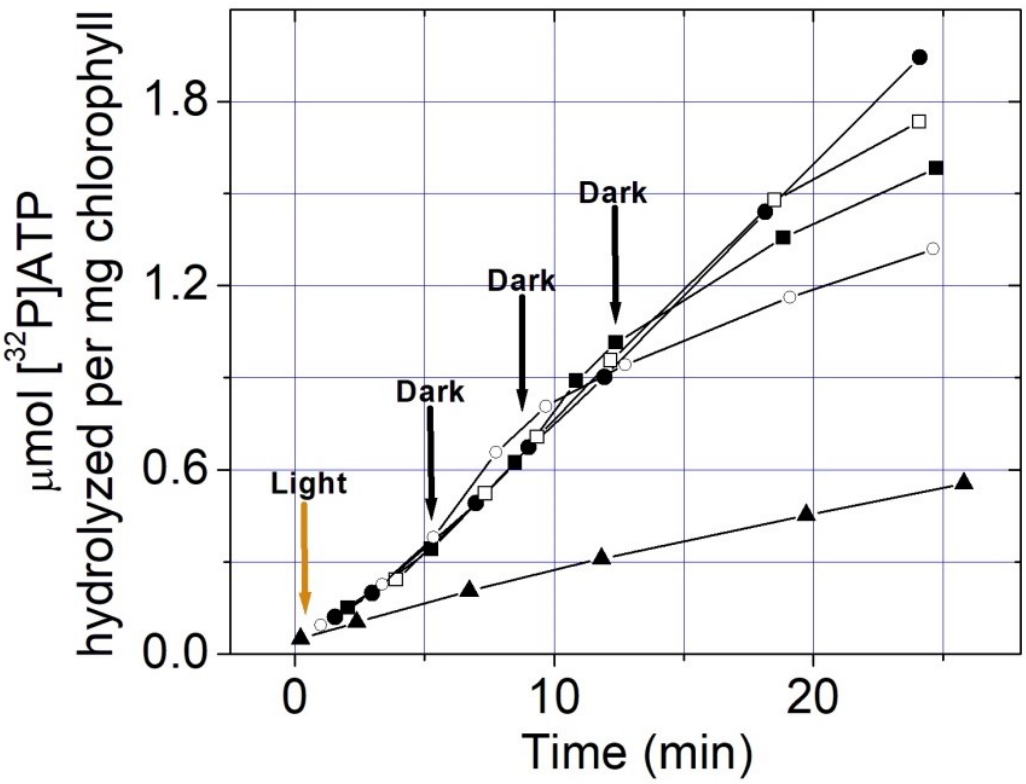

Figure 7: Light-triggered ATPase. ● – ●: *continuous light;* ○ – ○: *light turned off after 5.25 min;* ■ – ■: *light turned off after 8.50min;* □ – □: *light turned off after 12.25 min;* ▲ – ▲: *dark. Each reaction mixture contained, in a total volume of 6.0 ml, in* μmol: *Tris-HCl (pH7·8), 90; potassium phosphate (pH 7.8), 24; phenazine methosulphate, 0.2; potassium ascorbate, 60;* $MgCl_2$, *6;* NH_4Cl, *3; Uncoupler cysteine-HCl (pH 7.8), 500;* $[^{32}P]ATP$, *1.3 (containing* 1.2×10^6 *counts/min), and once washed chloroplasts containing* $54\mu g$ *of chlorophyll.*

Only the nucleoside triphosphates were hydrolyzed in the light. Considerable hydrolysis was observed in the dark. The light-triggered ATPase can also hydrolyze ATP, GTP and ITP.

But not any of the nucleoside diphosphates tried. It was reported the higher dark inorganic phosphate release that can be observed under the reaction conditions for the light-triggered ATPase.

In the presence of uncoupling conditions with $CaCl_2$ in the reaction mixture was shown a light-dependent change of CF_1 to function as ATPase. Also changes affinity for substrate and inhibitor.

The affinity of photophosphorylation for ADP and GDP was found to be similar under conditions optimal for photophosphorylation, but very different under conditions optimal for the light-requiring ATPases.

The affinity of the light-requiring ATPases for ADP and GDP as competitive inhibitors was found to be identical to the affinity of photophosphorylation for the compounds under the same experimental conditions.

Assay procedure for both ATPases: Fractions of 0.5 ml each were removed at the indicated times into 0.05 ml of 30% trichloroacetic acid for assay as previously described. The [^{32}P]ATP was prepared as previously described. Light intensity 100,000 lux; temperature 21°C [58] [59].

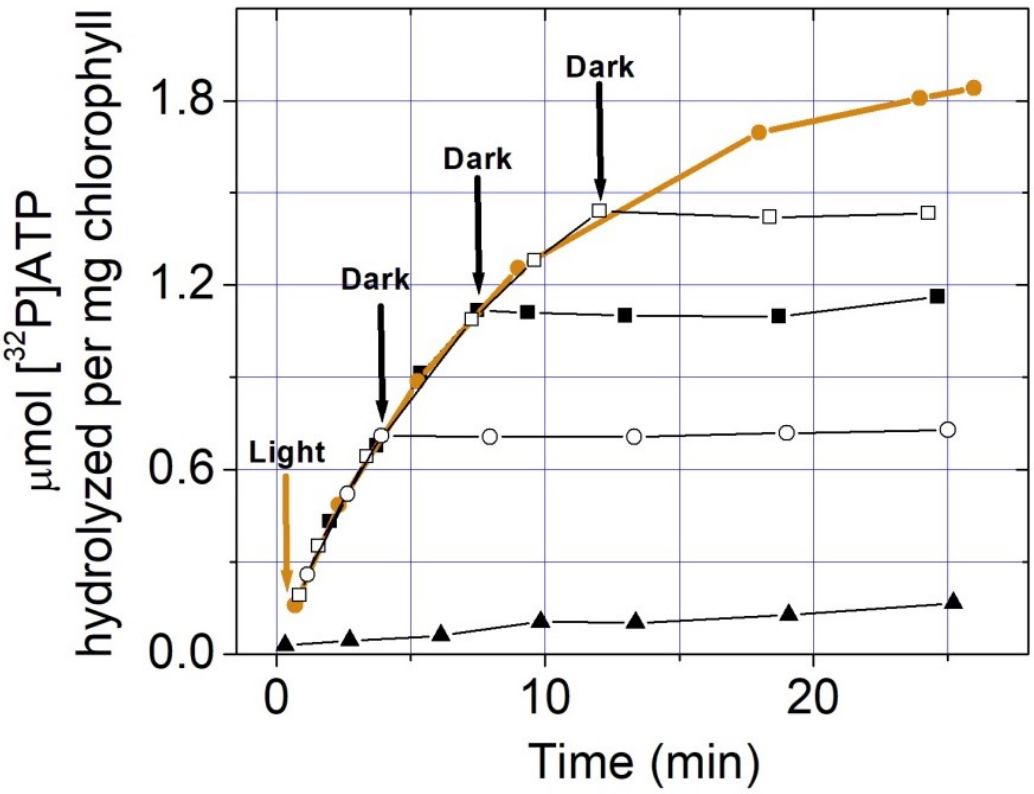

Figure 8: Light-dependent ATPase. *. ● — ●: continuous light; ○ — ○: light turned off after 4 min;* ■ — ■*: light turned off after 7.50min;* □ — □*: light turned off after 12.00 min;* ▲ — ▲*: dark. Each reaction mixture contained, in a total volume of 6.0 ml, in* μmol*: Tris-HCl (pH7·8), 90; potassium phosphate (pH 7.8), 24; phenazine methosulphate, 0.2; potassium ascorbate, 60;* $\underline{CaCl_2}$*, (uncoupler) 6;* $[^{32}P]ATP$*, 1.3 (containing* 2×10^6 *counts/min) and once washed chloroplasts containing* $86\mu g$ *chlorophyll.*

All tables reported the use of the same buffer: Each reaction mixture contained in a total volume of 3.0 ml, additions in µmol. The reaction was terminated The inorganic phosphate released was assayed by the method of Ernster et al. Reaction time 20 min; temperature 20°; light intensity 100,000 lux.

Table 1: Light-dependent ATPase. *Substrate specificity was assayed. Tris-HCl (pH 7.8), 75* μmol*; potassium phosphate (pH 7.8), 12* μmol*; phenazine methosulphate, 0.1* μmol*; potassium ascorbate (pH 7.8), 30* μmol*;* $CaCl_2$*, 3* μmol*; nucleotide, 0.6* μmol*; and once-washed chloroplast fragments containing 121 µg of chlorophyll.*

Substrate	Inorganic phosphate released $\mu mol/mg\ chl.h$	
	Light-dark	Dark
ATP	2.83	1.17
GTP	1.88	0.30
ITP	1.28	0.30
ADP	0.00	0.52
GDP	0.10	0.60
CDP	0.00	0.45
UDP	0.10	0.55

Table 2: Light-triggered ATPase. *Substrate specificity was assayed. Tris-HC1 (pH 7.8), 45 μmol; potassium phosphate (pH 7.8), 12 μmol; phenazine metasulphate, 0.1 μmol; potassium ascorbate, 30 μmol; $MgCl_2$, 3 μmol; NH_4Cl, 1.5 μmol; cysteine-HCl (pH 7.8), 250 μmol; nucleotide as indicated, 0.6 μmol; and once-washed chloroplast fragments containing 121 μg chlorophyll.*

Substrate	Inorganic phosphate released $\mu mol/mg\ chl.h$	
	Light-dark	Dark
ATP	2.9	3.2
GTP	1.1	0.0
ITP	0.65	1.2
ADP	0.0	3.0
GDP	0.0	0.75
CDP	0.0	0.50
UDP	0.0	1.57

The wide specificity for nucleoside triphosphates as substrates of the light-requiring ATPase of chloroplasts (Tables I and II) are similar to the wide specificity previously reported for other ATPase preparations.

Table 3: Determination of apparent constants. *K_i, K_m and V in light-dependent, light-triggered ATPases and photophosphorylation were assayed.*

Tabla 3: Determinación de constantes aparentes. *Se analizaron Ki, Km y Vmax en ATPasas dependientes de la luz, activadas por la luz y fotofosforilación.*

Reaction	Optimal conditions for	Kinetics constants	K_m	K_i	V_{max} μmol $/mg\ chl.h$
			$M \times 10^{-5}$		
Photophosphorylation	Photophosphorylation	ADP	6	-	700
		GDP	7	-	400
	Light-dependent ATPase	ADP	4	-	18
		GDP	50	-	14
	Light-triggered ATPase	ADP	4	-	500
		GDP	100	-	600
Light-dependent ATPase	Light-dependent ATPase	ATP	4	-	25
		ADP	-	3	-
		GDP	-	50	-
Light-triggered ATPase	Light-triggered ATPase	ATP	9	-	15
		ADP	-	4	-
		GDP	-	100	-

The wide specificity of the light-requiring ATPase to inhibition by nucleoside diphosphates is reported. The affinity for ADP and GDP as inhibitors of the light-requiring ATPases was found to be identical to the affinity for the same compounds as phosphate acceptors for photophosphorylation under the same experimental conditions.

The requirement for the coupling factor in the restoration by uncoupling of the activity of the light-requiring ATPases indicates that the site of action of the coupling factor must be located within that part of the energy-transport chain. Therefore, is common to both photophosphorylation and the

light-requiring ATPases. The small, but significant and repeatable dark ATPase activity of the coupling factor by itself, may indicate a potential masked ATPase activity, in a fashion analogous to the ATPase activity of some of the coupling factors isolated from mitochondria.

Table 4: Reactivation of photophosphorylation and light-requiring ATPases by addition of an isolated coupling factor (CF_1). *Recombination was performed by pre-incubation for 20 min at* $0°C$ *of EDTA fragments containing* $50\mu g$ *chlorophyll with the coupling-factor supernatant (*$50\mu g$ *of protein obtained from chloroplast fragments containing* $75\mu g$ *chlorophyll) and 6 mM $MgCl_2$ or $CaCl_2$ for the light-triggered or light-dependent ATPases, respectively. Chloroplast fragments containing* $50\mu g$ *of chlorophyll and coupling factor containing* $50\mu g$ *protein were used in each reaction mixture, where indicated. Reaction time 10min; light intensity 100,000lux; temperature 20°C.*

Additions reaction mixture for the respective assays	Photophosphorylation		Light-dependent ATPase $[^{32}P]ATP$ hydrolysed			Light-triggered ATPase $[^{32}P]ATP$ hydrolysed		
	ATP synthesized (μmol $/mg\ chl.h$)	Original %	Light-dark (μmol $/mg\ chl.h$)	%	Dark (μmol $/mg\ chl.h$)	Light-dark (μmol $/mg\ chl.h$)	%	Dark (μmol $/mg\ chl.h$)
Intact fragments	512	100	3.50	100	0.26	2.12	100	0.57
EDTA extracted fragments (E)	0	0	0.03	1	0.03	0.01	0	0.16
Recovered function E plus CF_1	40	8	0.27	8	0.10	0.19	9	0.20
Coupling factor (CF_1)	-	-	0.00 **[*]**	0	0.03 **[*]**	0.00	0	0.05
[*] Expressed as μmol per 1.5mg coupling factor protein per h.								

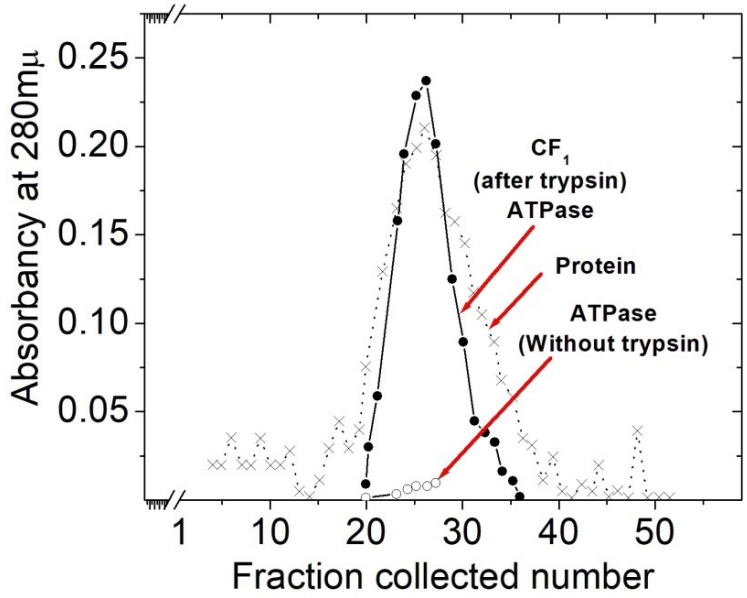

Figure 9: Purification of latent ATPase (CF_1) on DEAE-Sephadex chromatography column. *About 190 mg of CF_1 extracted from chloroplasts, containing about 1,000 units of latent ATPase were fractionated on DEAE-Sephadex. To the fractions, ATP was added to a final concentration of 2 mM (in order to protect the active center and prevent the denaturation), and solid ammonium sulfate was added to yield a 2 M solution. On elution an inactive protein was obtained and reactivated on storage in 2.0 M ammonium sulfate containing 2 mM ATP stored at 4°C. After 24 hours aliquots of the suspension were centrifuged, and the precipitate was dissolved in 5 mM Tris-Cl, pH 8.0, and assayed for protein (spectrophotometrically) and treated to manifest ATPase activity before and after trypsin treatment.*

All of the reported findings strongly support the coupling factor CF_1 that has latent both of the high light-requiring ATPases. Activities found in isolated chloroplasts involved a single protein as shown by the purified protein CF_1, when treated with trypsin revealed that has activated a latent ATPase function. Accordingly, CF_1 is the only responsible for the terminal step of ATP formation during the activity of the photophosphorylation system.

It was shown with tritium-labeled CF_1 that a divalent cation such as Mg^{2+} or Ca^{2+} was required for the binding of the protein to the chloroplast membrane.

Treatment of tritium-labeled acetyl-CF_1 with trypsin or heat activated a Ca^{2+}-dependent ATPase. However, this procedure abolished the capacity of CF_1 to combine with resolved chloroplast particles.

On extraction of chloroplasts with solvents, two fractions, one a soluble protein CF_1 and one insoluble membrane fragment, were separated. Both fractions by mixing and stored in the cold were able at a posterior step to reconstitute particles, which were able to manifest allotopic properties.

Discussion

The Big-Bang allows characterizing the expansion with the fundamental property of bosons quantum entanglement, because they occupy the same quantum state.

The bosons do not respond to the Pauli exclusion's principle, which allows these maximal nodes of energy. Thus, in opposition to the fermions allowed localizing into singular multi-levels of energy. Thus, separating the continuum of causality and the entanglement, could define quantum parameters of chemical bonding configurations for atoms and molecular structures.

After the Dark Ages, the surging stars emit not only thermal photons, which lack response to gravity, but also the ones produced by internal nuclear hydrogen fusion into helium and radiated from the star's surface, which does respond to gravity, the star's mass is dissipated by radiation. The cosmological model assumed was to postulate a gyroscopic capacity of the Universe rotational state, functioning for feedback regulation of flatness.

Prigogine modeled from transfer of a larger to a smaller system to increase enthalpy in the smaller one, allowing life as an open system, showing an entropy dilution. However, his model was not dissipative but based on a tendency for mass action equilibrium between enthalpy and entropy. The model postulated in this work the thermodynamics treatment of structure and function allowed the architectural separation from enthalpy from entropy. This one requires enthalpy intake maintaining high potential continuous work and the generated entropy to be rapidly and continuously release from the system that has been referred as a dissipative state. Thus, implicates a thermodynamics differential by structure and function separating enthalpy and entropy pathways.

Common knowledge describes a thermodynamics system as open to the sun and integrated to life dependent from H_2O [60]. The confluence of requirements should be evident in terms that the sun evaporates water clusters: $(H_2O)_n$ by separating the molecules integrated in the complex and day-cycle allows the cooling for the vapor condensing as rain and returning spontaneously to the water cluster state. In the brain the dissipative pathway for entropy allows the water dimers: $H_2O{\sim}OH_2$, containing the heat as resonance states that when reach the oral cavity will evaporate.

The water cluster could couple for conformational change involving the hydrophilic to hydrophobic structural modification of protein dynamic. The hydrophilic state is associated to a coordinated Me^{2+} attracted to negative R groups and amphoteric histidine. The acting dynamics between two forms on of proteins and DNA by H-bonds breakdown could change configuration, characterized in a *mutual exclusion* preventing that two structural forms could not exist simultaneously, in order to differentiate the functional state. Example: the oxyHb vs deoxyHb. Likewise, it ensures cyclic vectoriality (*turnover*) to the entire function.

The presence of the proline in the polypeptide chains [61] allows folding and displacement allows the reconversion from hydrophilic to hydrophobic domains. Hence, allowing create the hydrophobic domain by allowing amphoteric His groups and complemented by positive R groups to create attraction for bonding negative molecules, like 2,3–DPG^{5-}, ADP^{3-}, etc. Thus, configures a hydrophobic or less polar state. The hydrophilic to

hydrophobic state maintains vectoriality by turnover, not allowing a direct return but recreating a new initial state.

Thus, increasing rotational and vibrational kinetic activity, on the separated individual H_2O molecules, but maintaining a liquid coherence, during circulation within astrocytes until the lower pressure at the vomeronasal organ (VNO) [62] [63] allows phase conversion to vapor, equivalent to entropy dissipation. The sum of the energy generated by metabolites and H-bond consumption allows the brain thermodynamics to support high ratios between metabolite concentrations and the electrogenic action potential in the dissipative states, within an open system.

The dissipative thermogenic H-bonds breakdown within water cluster configures a randomness increment when coupled to the proline-dependent folding of a polypeptide, but under experimental conditions the potential of an irreversible process would be undetectable because the protein concentrations could be µM whereas the mass-action of environmental water cluster would be several millions higher.

Malate enters the chloroplasts and is oxidized and decarboxylated (loses CO_2) by malic enzymes. This yields high concentrations of carbon dioxide, which is fed into the Calvin-Benson cycle of the bundle sheath cells, and pyruvate, a three-carbon acid that is translocated back to the mesophyll cells.

Conclusions

Solar energy has through the water states of aggregation the manifestation of life on earth.

Photosynthesis sustains virtually all life on planet Earth providing the oxygen we breathe and the food we eat; it forms the basis of global food chains and meets the majority of humankind's current energy needs through fossilized photosynthetic fuels. The process of photosynthesis in plants is based on two reactions that are carried out by separate parts of the chloroplast.

The hydration shells could sequence enhanced activation energy (Ea) into several peaks, to sequentially activate transition states. Hence, changes in dipole state, sliding, pKa, n-H-bonds, etc., could become concatenated for vectoriality. $(H_2O)n$ by the loss of H-bonds coupled with the hydration turnover of proteins and ions to result in incomplete water cluster $(H_2O)n^*$, with a lower-n. $(H_2O)n^*$ became a carrier of heat/entropy.

The dissipative potential of water clusters $(H_2O)_n$ interacts with the hydrophilic vs hydrophobic asymmetries to restrict randomness of the kinetic sense implicated in a single peak for Ea.

Due to the magnetoresistance effect, the neuron converts the modulations of the current into a variation of the voltage between its terminals.

The cycle of water from vapor to rain also couples with photosynthesis, a process that releases the oxygen from water and hydrogen appears in the oxidation-reduction NADPH carrier cycles which reduce oxaloacetate to malate allowing to incorporate CO_2 into the Calvin's cycle, or photosynthetic carbon reduction (PCR) cycle, of photosynthesis are the chemical reactions that convert carbon dioxide and hydrogen-carrier compounds into glucose.

The agricultural yield dependence of photophosphorylation could be optimized by addition of Mg^{2+} and decreasing Ca^{2+} and other uncouplers or inhibitors. Hydroponics crops efficiency as well in terrains could be improved by addition of potassium phosphate as buffer to obtain the desired pH for every vegetable. This irrigation water could be used for desalination of desert spots creating mini-fields optimal for the specific water needs of each crop.

Poor nations may replace the urea by using NH_4Cl or even better by NH_4NO_3 as fertilizers. Seawater desalination process if implies to expensive production plants should be imported from other countries under the specification that would be used for agriculture purposes. That could reduce the costs by the additions, which will dilute residual salinity by introducing ammonium to form NH_4Cl.

The phenazine methosulfate used to potentiate photophosphorylation in spinach chloroplast to maximize ATP yields will require specific studies for each crop.

The production of artificial light at night could add significant farming yields, especially at Polar Regions with not adequate sunlight.

Transmitted letter to NASA describes the generation of light from scintillation crystals mixtures covering the radioisotopes Sr-89 half-life 90 days and Sr-90 half-life 30 years [64]. Thereafter the emission of light received by photovoltaic cells

to produce electricity resulted in additional publications [65] [66] [67]. The beta (electron) disintegration by Sr-89 produces photon emission by scintillators crystals and therefore a secure shielding. Therefore both radioisotopes provide efficient beta-scintillator batteries, but the Sr-90 is adaptable to Mars colonization purposes.

The up and down of the spin-flip shift in the electron orbital of H could be linked to a vibrational transition in the Fermi energy levels. The emitted energy in the 21 cm line dominated the Dark Ages of the Universe and that corresponds to the linear impulse (momentum), showing redshift due to expansion (intergalactic distancing). The Milky Way and Andromeda have a spatial approach course with a blue shift [68] [69].

In the Big-Bang, the primordial gravitational waves (space-time oscillations) with an expansion trajectory originate a high elastic resistance (limiting) to space expansion due to velocity c on the self-contained universe border that could correspond to a higher density of dark matter [70] [71].

The enthalpy transformation thermodynamics produces entropy (thermal waves) that is located internally in the voids and exerts pressure, preventing galactic scattering, which characterizes the dark energy.

The oscillatory stage against the shell fixes the translation dimensions of the primordial Big-Bang gravitational waves, expanding vectorially to the outline of the universe as a self-contained (high resistance) fixed shell.

Predictions from the cosmological models and the eBoss project reveal several features, each of which are caused by different physical processes. Thus, a variation at a single scale in which the density of the primordial plasma varies with position like a simple sinusoidal wave. The amplitude of the fluctuations between the most and least dense regions will change with time under the influence of two forces pressure that acts in the opposite of gravity, driving material out of dense regions and reducing the size of the density difference.

The relationship of energy flows operated on Fermi description of a layered structuring free layer of fermions (matter), operating during expansion. The space evolution of chronological dispersion is generated by bosons. The amount of energy required to re-orient the magnetization of the system into two anti-aligned fermions vs bosons could be calculated from perceptual values presently attributed.

An electron entrained in the plasma "sees" the surrounding primordial plasma moving toward it with different velocities: faster from the left and the right, but slower from above and below. Consequently, the relative velocities have a quadrupole moment, in the intensity of the incident radiation, since the plasma was moving at high speeds the relativistic effects emerge, as a faster the plasma, the brighter will appears. Hence, there is a quadrupole moment on the electron and the radiation scattered by the charged particle has a polarized component, contributing to energy space localization.

Quantum entanglement could be part of thermodynamics flow from enthalpy to entropy across the chronology of the universe in a close state to function as open, has to create a dissipative space-time locus. Accordingly, this localization will correspond to voids that function in an expanding phase as pressure to propel galaxies toward the redshift direction of the visible wavelength spectrum, decreasing the density of energy by expansionary effect of cooling. Residual to the enthalpy expenses location emerging as entropy of the impulse motion of stars and galaxies.

In 2021, data from NASA's New Horizons space probe was used to revise the earlier estimate to roughly 200 billion galaxies (2×10^{11}).

The very large size of the voids indicates capability that their momentum photons localization pressure, could partition of momentum inwardly and to outside pressuring the galactic contour, decreasing of frequency by cooling enlarging photon location and produces its own pressure. Consequently, the linear impulse to propel matter increases momentum (p) to approach infinite. Hence fore, their partition of momentum requires increases of angular momentum.

Gyroscopic movement of the universe provides feedback for the system, maintaining flatness curvature. The velocity of the universe increase could not exceed gravitational waves relativistic considerations are that void pressure (or equivalent momentum) approaches a value antagonistic with gravity. Accordingly, to Einstein its solution for cosmological constant and since other values has to adjust the proposed values for

voids pressure (Dark Energy) vs mass pressure (Dark matter) for expansionary border of the universe.

References

[1] Cardona, T., Sedoud, A., Cox, N. and Rutherford, A. W. Charge separation in photosystem II: a comparative and evolutionary overview. Biochim Biophys Acta 1817(1), 26-43 (2012 Jan).

[2] Penrose, R. and Hameroff, S. Consciousness in the universe: a review of the 'Orch OR' theory. Phys Life Rev., 11(1), 39-78 (2014 Mar).

[3] Hameroff, S.. Consciousness, Neurobiology and Quantum Mechanics. In Tuszynski, Jack (ed.). The Emerging Physics of Consciousness (2006).

[4] "Can Quantum Physics Explain Consciousness? One Scientist Thinks It Might". Discover Magazine. Archived from the original on 3 October 2020. Retrieved 7 October 2020.

[5] Tegmark, Max. The importance of quantum decoherence in brain processes. Physical Review E. 61 (4): 4194–4206 (2000). arXiv:quant-ph/9907009.

[6] Bennun, A. The Human Oral-Cavity-NA-AC-Hypothalamic axis on the developing of emotional intelligence, creativity and innovation. viXra.org > Biochemistry > viXra:2111.0157 (2021-11-29).

[7] Bennun A. The dynamics of H-bonds of the hydration shells of ions, ATPase and NE-activated adenylyl cyclase on the coupling of energy and signal transduction. https://arxiv.org/abs/1208.5673 [q-bio.OT] (2012).

[8] Zhu, X-G., Govindjee, Baker N.R., Ort, D.R. and Long, S.P. Chlorophyll a fluorescence induction kinetics in leaves predicted from a model describing each discrete step of excitation energy and electron transfer associated with Photosystem II. Planta. 223(1), 114-133 (2005).

[9] Vos, M.H., Rappaport, F., Lambry, J.C., Breton, J. and Martin, J.L. Visualization of coherent nuclear motion in a membrane protein by femtosecond spectroscopy. Nature, 363, 320 (1993).

[10] Yakovlev, A.G., Shkuropatov, A.Y., Shuvalov, V.A. Nuclear wavepacket motion producing a reversible charge separation in bacterial reaction centers. FEBS Lett. 466(2-3), 209-12 (2000 Jan 28).

[11] Streltsov, A.M., Yakovlev, A.G., Shkuropatov, A.Y. and Shuvalov, V.A. Femtosecond kinetics of electron transfer in the bacteriochlorophyllM-modified reaction centers from Rhodobacter sphaeroides (R-26). FEBS Letters, 383(1–2), 129-132 (1996 March 25).

[12] Vos, M.H., Jones, M.R., Hunter, C.N., Breton, J., Lambry, J.C. and Martin, J.L. Coherent dynamics during the primary electron-transfer reaction in membrane-bound reaction centers of Rhodobacter sphaeroides. Biochemistry, 33(22):6750-7 (1994 Jun 7).

[13] Arnett, D.C., Moser, C.C., Dutton, P.L. and Scherer, N.F. The first events in photosynthesis: electronic coupling and energy transfer dynamics in the photosynthetic reaction center from rhodobactersphaeroides. J. Phys. Chem. B, 103, 11, 2014-2032 (1999).

[14] Emerson, R. and Arnold, W. The photochemical reaction in photosynthesis. J. Gen. Physiol. 16, 191-205 (1932).

[15] Bennun, A. and Ledesma, N. The photon structure in interference processes, Quantum Entanglement and Self-Organized Cosmos. viXra.org > Relativity and Cosmology > viXra:2109.0214 (2021-09-30).

[16] Jha, A.K., Malik, M. and Boyd, R.W. Exploring energy-time entanglement using geometric phase. Phys. Rev. Lett. 101, 180405 (2008).

[17] Brunner, N., Cavalcanti, D., Pironio, S., Scarani, V., Wehner, S. Bell nonlocality. Rev. Mod. Phys. 86(2):419-478 (2014). arXiv:1303.2849.

[18] Werner, R.F. Quantum States with Einstein-Podolsky-Rosen correlations admitting a hidden-variable model. Physical Review A. 40 (8): 4277-4281 (1989).

[19] Bennun, A. Quantum state transition from liquid to vapor water by physiological entanglement. viXra.org > Biochemistry > viXra:2106.0053.

[20] Bennun, A. Simulation of the dynamics of integration of space-time-energy by Planck's temperature black body emission spectrum. viXra.org > Relativity and Cosmology > viXra:2008.0210.

[21] Vedral, V. and Plenio, M.B. Entanglement measures and purification procedures. Phys. Rev. A 57, 1619 (1998).

[22] Franson, J.D. Bell inequality for position and time. Phys. Rev. Lett. 62, 2205 (1989).

[23] Kwiat, P.G., Steinberg, A.M. and Chiao, R.Y. High-visibility interference in a Bell-inequality experiment for energy and time. Phys. Rev. A 47, R2472 (1993).
[24] Brendel, J., Mohler, E. and Martienssen, W. Time-resolved dual-beam two-photon interferences with high visibility. Phys. Rev. Lett. 66, 1142 (1991).
[25] Jha, A.K., O'Sullivan, M.N. Chan, K.W.C. and Boyd, R.W. Temporal coherence and indistinguishability in two-photon interference effects. Phys. Rev. A 77, 021801(R) (2008).
[26] Takesue, H. and Inoue, K. Generation of polarization-entangled photon pairs and violation of Bell's inequality using spontaneous four-wave mixing in a fiber loop. Phys. Rev. A 70, 031802 (2004).
[27] Mandel, L. Coherence and indistinguishability. Opt. Lett. 16, 1882 (1991).
[28] Werner Heisenberg, Encounters with Einstein and Other Essays on People, Places and Particles, Published October 21st 1989 by Princeton University Press,p.53.
[29] Howell, J.C., Bennink, R.S., Bentley, S.J. and Boyd, R.W. Realization of the Einstein-Podolsky-Rosen paradox using momentum- and position-entangled photons from spontaneous parametric down conversion. Phys. Rev. Lett. 92, 210403 (2004).
[30] Rarity, J.G. and Tapster, P.R. Experimental violation of Bell's inequality based on phase and momentum. Phys. Rev. Lett. 64, 2495 (1990).
[31] Beth, R.A. Mechanical Detection and Measurement of the Angular Momentum of Light. Phys. Rev. 50, 115 (1936).
[32] Allen, L., Beijersbergen, M.W., Spreeuw, R.J.C. and Woerdman, J.P. Orbital angular momentum of light and the transformation of Laguerre-Gaussian laser modes. Phys. Rev. A 45, 8185 (1992).
[33] Jha, A.K., Jack, B., Yao, E., Leach, J. Boyd, R.W., Buller, G.S., Barnett, S.M., Franke-Arnold, S. and Padgett, M.J. Fourier relationship between the angle and angular momentum of entangled photons. Phys. Rev. A 78, 043810 (2008).
[34] Sinatra, A., Castin, Y. and Witkowska, E. Coherence time of a Bose-Einstein condensate. Phys. Rev. A 80, 033614 (2009).
[35] Ladd, T.D., Maryenko, D., Yamamoto, Y., Abe, E. and Itoh, K.M. Coherence time of decoupled nuclear spins in silicon. Phys. Rev. B 71, 014401 (2005).
[36] Ivanov, A.G., Öquist, G., Hüner, N.P.A.. Thermoluminescence. Photosynthesis pp 445-474 (2011 August).
[37] Locatelli, N. et al. Spintronic devices as key elements for energy-efficient neuroinspired architectures. Proceeding of the 2015 Design, Automation & Test in Europe Conference & Exhibition, 994-999 (2015).
[38] Grollier, J. et al. Neuromorphic spintronics. Nature Electronics, 3, 360-370 (2020 July).
[39] Engel, G.S., Calhoun, T.R., Read, E.L., Ahn, T.K., Mancal, T., Cheng, Y.C., Blankenship, R.E. and Fleming, G.R. Evidence for wavelike energy transfer through quantum coherence in photosynthetic systems. Nature, 446, 782-786 (2007).
[40] Bennun, A. and Racker, E. Partial resolution of the enzymes catalyzing photophosphorylation IV. Interaction of coupling factor I from chloroplast with components of the chloroplast membrane, The Journal of Biological Chemistry, 244, 1325-1331 (1969).
[41] Stoppani, A.O.M., Bennun, A. and De Pahn, E.M. Effect of DNP on the metabolism of phosphates in Saccharomyces cerevisiae, "5th inter-American Symposium on the Peaceful Application of Nuclear Energy" in Symposium sponsored by the inter-American Nuclear Energy Commission and the Goverment of Chile, Valparaíso, Chile, 1964, J.D. Perkinson and the Secretariat of IANEC, (1965), pp. 59-68, Organization of American States, Washington, D.C.
[42] Stoppani, A.O.M., Bennun, A. and De Pahn, E.M., Energy requirement for the anaerobic oxidation of acetate in baker's yeast, Biochimica et Biophysica Acta, 92, 176-178 (1964).
[43] Bennun, A., De Pahn, E.M. and Stoppani, A.O.M., Some properties of particle-bound intracellular ATPase from baker's yeast, Biochimica et Biophysica Acta, 89, 532-539 (1964).
[44] Stoppani, A.O.M., Bennun, A. and De Pahn, E.M. Effect of 2,4-dinitrophenol on Krebs cycle and phosphate metabolism in baker's yeast, Archives of Biochemistry and Biophysics. 108(2), 258-265 (1964).

[45] Kramer, D.M. and Evans, J.R. The importance of energy balance in improving photosynthetic productivity. Plant Physiology, 155(1), 70-78 (January 2011).
[46] Bennun, A. Interacción de factor acomplante del cloroplasto con protones y agua. Recientes Adelantos en Biologia (página 254) Editores Raul H. Megia y Jaime A. Moguilevsky, simposia Buenos Aires, 1971 (Titration with glycerol allow to determine the number of water molecules involved in the turnover of the active site of CF1-ATPase).
[47] Bennun A. The coupling of thermodynamics with the organizational water-protein intra-dynamics driven by the H-bonds dissipative potential of water cluster. https://arxiv.org/abs/1303.6993.
[48] Bennun A. The assay of the hydration shell dynamics on the turnover of the active site of CF1-ATPase. Book Title: Advances in Chemistry Research. Volume 33, chapter 8. Editor James C Taylor. Nova Publishers (2016). https://novapublishers.com/shop/advances-in-chemistry-research-volume-33
[49] Bennun, A. The assay of the hydration shell dynamics on the turnover of the active site of CF1-ATPase. Arxiv. 7 Jul 2016. https://arxiv.org/abs/1611.00716
[50] Bennun, A. Hypothesis for coupling energy transduction with ATP synthesis or ATP hydrolysis, Nature New Biology, 233, (1971), No. 35, 5-8.
[51] Bennun, A. and Bennun, N. Hypothesis for a mechanism of energy transduction. Sigmoidal kinetics of chloroplast's heat-activated ATPase, Proceedings 2nd International Congress on Photosynthesis Research (G. Fortí, M. Avron and A. Melardri, eds.), 2, 1115-1124, (1972). Dr. W. Junk N.V. Pub., The Hague.
[52] Bennun, A. The unitary hypothesis on the coupling of energy transduction and its relevance to the modeling of mechanisms, Annals of the New York Academy of Sciences, 227, 116-145 (1974).
[53] Bennun, A. Hypothesis on the role of liganded states of proteins in energy transducing systems, Biosytems, 7, 230-244 (1975).
[54] Bennun, A., A model mechanism for coupled phosphorylation, Proceedings 3rd International Congress on Photosynthesis, Rehovoth (M. Avron, ed.), (1974), Vol. 2, pp. 1107-1120, Elsevier Sciences Pub. Co., Amsterdam.
[55] Bennun, A., Properties of chloroplast's coupling factor-1 and a hypothesis for a mechanism of energy transduction, Proceedings First European Biophysics Congress, Baden, Austria, 1971, in "Photosynthesis, bioenergetics, regulation, origin of life" (E. Broda, A. Locker and H. Spríinger-Lederer, eds.), (1971), Vol. IV. pp. 85-91, Wiener Medizinischen Akademíe, Vienna.
[56] Bennun A. Interaccion de factor acomplante del cloroplasto con protons y agua. Recientes Adelantos en Biologia (página 254) Editores Raul H. Megia y Jaime A. Moguilevsky, simposia Buenos Aires, 1971 (Titration with glycerol allow to determine the number of water molecules involved in the turnover of the active site of CF1-ATPase).
[57] Bennun, A. Interaction of the chloroplast coupling factor with protons and water, Congreso Argentino de Ciencias Biológicas - 1970, in "Recientes adelantos en Biología" (J.A. Moguilevsky and R. Mejía, eds.), (1971), pp. 254-264, University of Buenos Aires Press.
[58] Bennun, A. and Avron, M., The relation of the light-dependent and light-triggered adenosine triphosphatases to photophosphorylation, Biochimica et Biophysica Acta, 109, 117-127 (1965).
[59] Bennun, A. and Avron, M. Light-dependent and light-triggered adenosine triphosphatases in chloroplasts, Biochimica et Biophysica Acta, 79, 646-648 (1964).
[60] Bennun, A. The Thermodynamic Inwardly Open System by Locally Decreasing Entropy Originates Life. viXra.org > Relativity and Cosmology > viXra:2104.0155 https://vixra.org/abs/2104.0155 (2021-04-25).
[61] Bennun, A. The imidazole ring of proline allows a polypeptide folding dynamics by H-bonds breakdown sliding for a vectorial exergonic hydrophilic to an endergonic hydrophobic configuration for Hb and active site functions. viXra.org > Biochemistry > viXra:2201.0182 (2022-01-26).
[62] Trotier, D. Vomeronasal organ and human pheromones. European Annals of Otorhinolaryngology. Head and Neck Diseases, 128 (4), 184-190 (2011).
[63] Bennun, A. The regenerative processes involving the cAMP unzipping of DNA. The synthesis of proteins integrating plasticity and

longevity. Biochemistry Research Trends. Book Published by Nova Biomedical, Copyright 2017 by Nova Science Publishers, Inc.
[64] Bennun, A. Integrative design for radio nuclear power-transfer by light to batteries. Phase I – Advanced Aeronautical/Space Concept Studies – NIAC CP 05-01. NASA. (Submission date: 2005 Feb 5).
[65] Bennun, A. Recovery of radioisotopes from nuclear waste for radio-scintillator-luminescence energy applications. arXiv, physics, general physics, https://arxiv.org/abs/1208.3502 [physics.gen-ph] (2012).
[66] Bennun A. and Ledesma N. Advances in the efficiency of beta-scintillator batteries and its adapting to support electric vehicles. Book Series: International Journal of Energy, Environment, and Economics. Volume 23, Number 1 (pages: 41 to 52) 2015.
[67] Bennun A. Recovery of radioisotopes from nuclear waste for radio-scintillator-luminescence. Energy applications. International journal of energy, environment, and economics. ISSN: 1054-853X, Vol. 20, No 5, pp. 509-515, 2012, Nova Science Publishers, Inc.
[68] Bennun A. Book: The brain structures micro to nano space-time levels into the thermodynamics of an open-system. Editorial: Amazon (October 28, 2022) ISBN-13: 979-8360732990.
[69] Bennun A. El cerebro estructura los niveles de micro a nano del espacio-tiempo en su funcionamiento como un sistema termodinámico abierto. Editorial: Amazon (1 Diciembre, 2022) ISBN-13: 979-8366534031.
[70] Bennun, A. Book: Thermodynamics structuring of the universe. Editorial: Amazon (February 1, 2021) ISBN-13: 979-8706660116.
[71] Bennun, A. Libro: Estructuración termodinámica del universo. Editorial: Amazon (16 Junio, 2021) ISBN-13: 979-8521552344.